South Eastern Australian
Climate initiative

Final report for Project 2.2.3a

Develop improved regional projection techniques for MDB and the CMA regions of Victoria using multi-model weighted approach

Principal Investigator: Ian Smith

CSIRO Marine and Atmospheric Research, ian.smith@csiro.au, PMB 1, ASPENDALE, VIC, 3195, Ph: 03 9239 4400 Fax: 03 9239 4444

Co-Authors: Ian Watterson Penny Whetton

CSIRO Marine and Atmospheric Research, ian.watterson@csiro.au, penny.whetton@csiro.au PMB 1, Aspendale, VIC, 3195, Ph: 03 9239 4400 Fax: 03 9239 4444

Completed: 30 June 2007

Abstract
In response to stakeholder demands for both less uncertain regional climate change predictions and probabilistic information, new methods have been developed for synthesizing the results from numerous climate model experiments. This report describes a new method for generating probability density functions for scaled warming and net warming for points over south-east Australia. The method allows for weighting of different model results and has been demonstrated using the results from four models. In addition, a method for weighting different model results has also been developed and this is demonstrated using the results for rainfall for the Murray Darling Basin region from 22 models. Project 2.2.3b will demonstrate the results of the application of these new methods to the key regions.

Significant research highlights, breakthroughs and snapshots

- A trial set of probability distributions for DJF temperature change at a grid point in the vicinity of the MDB indicates a mean net warming of about +4.0^{o}C at 2100.

- Results also indicate that severe weighting, based on model performance criteria, can result in a significantly different mean response for MDB rainfall than that based on equal weighting of all model results. Preliminary results indicate the mean response is much drier.

- There is now an increasing recognition amongst the research community of the importance of careful assessment of climate model simulations before their results are used in impacts studies. This was refelected in feedback from a Climate and Hydrology Symposium recently held in Canberra where some of this work was reported.

Statement of results, their interpretation, and practical significance against each objective

Objective 1: To develop new methods for projections for the MDB and the CMA regions of Victoria using a multi-model weighted approach.

The technique for developing probability distributions is sufficiently general to be extended to a larger set of model results and other variables. It will be used to produce a new set of Australia-wide set of projections based on the IPCC Fourth Assessment Report model results.

Objective 2:

To provide information in response to stakeholder feedback which indicate a preference for probabilities.

The results indicate that estimates for the 5% and 95% confidence thresholds for DJF arming at 2100 are about +2.8 ^{o}C and +3.2 ^{o}C respectively.
They also indicate a potentially significant shift in derived probabilities for rainfall projections. These appear to be much less uncertain than previously shown. This will be further examined as part of Project 2.3.b.

1. Background

Projections at regional scales tend to be accompanied by relatively large uncertainties due to differences in model formulations, resolution, and simulated responses combined with differences in possible future emission scenarios (CSIRO, 2006; Whetton et al, 2005). Model developments, including improved physical parameterizations and the use of higher spatial resolutions, plus more simulations (i.e. the creation of multi-model ensembles) can potentially improve the reliability of regional scale results but it is apparent they will always be accompanied by some level of uncertainty.

Recently, regional rainfall projections produced by Whetton et al. (2005), CSIRO (2006) and Suppiah et al. (2007) used methods similar to those described Giorgi and Mearns (2002) in which a range of model results are sorted according to how well they represent features of the present day climate, but the projections simply presented as ranges of (equally likely) outcomes. Even so, the ranges remained relatively wide, particularly for south-eastern Australia (SEA), and there was not a great deal of difference between these and the previous projections based on fewer models and less stringent criteria (CSIRO, 2001). Stakeholders would like to see uncertainty minimized if possible and/or to have it quantified in a more useful fashion (i.e. generally in the form of probabilities or, more specifically, probability density functions (PDFs)). This is evident from key messages which emerged from a recent survey of focus groups ("2007 climate change projections for Australia: stakeholder feedback"):

- Generally, stakeholders are interested in the best case scenario, the worst case scenario, the most likely scenario and business as usual
- Likelihood is an important factor, so including probabilities is essential
- Stakeholders want to be able to compare 2007 projections with 2001 projections and with observations
- Stakeholders want regional information

For the Third Assessment Report (IPCC, 2001) there were 15 sets of model results available for preparing projections but 23 sets of results were available for the Fourth Assessment Report (AR4) (IPCC, 2007).

In this report we describe and demonstrate a method for generating probabilistic information.
This approach forms the basis of the new CSIRO/BoM climate change projections to be released later this year (Watterson, 2007). In addition we also describe and demonstrate a method for weighting the various model results. Appendices 1 and 2 contain further details of these methods.

2. Generating probabilistic climate change projections

The main aim is to provide a confidence weighting throughout the range of change considered plausible, basing this on the data from simulations by a number of current climate models. For most quantities this means, in effect, a 'probability density function' (PDF) for the change variable. Several recent studies have provided such results based on various approaches and assumptions, often of considerable complexity. A new, relatively simple method, has been applied to the results from

four models to produce surface warming projections for a point over south east Australia.

A number of methods for generating a PDF for scaled warming are illustrated in Fig. 1. Allowing for statistical uncertainty, the true value for each model (from multiple runs) is assumed to be from a simple normal PDF centred on the sample value. The uncertainty is determined from that appropriate to differences of two 30-y means, assuming these follow from the interannual standard deviation (SD) field, then scaled. The weighted sum of the four individual distributions is the 'Sum' PDF in Fig 1. (Weights used here are described in Appendix 1.) The normal distribution fitted to this Sum curve is also shown (as Normal). The beta distribution fit to the Sum curve is also shown. The 'Uniform' distribution is between the smallest and largest of the four change ratios. The final curve 'Narrow' is a normal fit to Sum, but with the SD reduced by the square root of the 'effective number of models'. This distribution would be appropriate if one considered the various model results to be a sample from a normal distribution centred on the 'true' change.

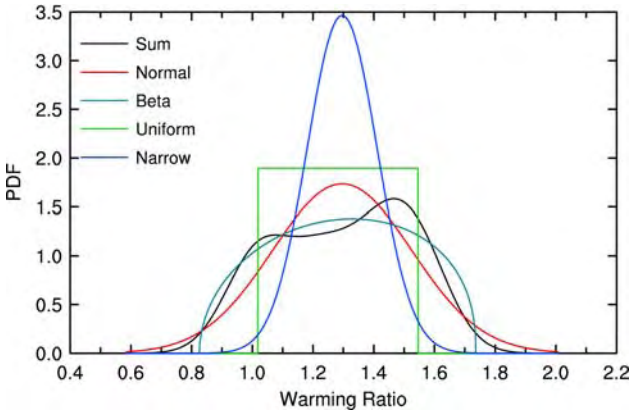

Figure. 1. Probability distribution functions for the warming ratio (local to global average warming) at a point over southeast Australia.

The warming ratio needs to be combined with the actual global mean warming (with its associated uncertainty) to produce a net change. The assumption is made that the scaled local change and the global warming are considered two independent variables. The joint distribution function is simply the product of the two PDFs. Statistics of the net local change can be determined numerically from this joint function.

For the A1B scenario in 2100, a value global average warming of around 3 K (or °C) is suggested by models. If, for simplicity it is assumed to be exactly 3K (i.e. SD=0.0 K), then the joint PDF for the local warming has the same shape as the scaled warming PDF. If the global warming is uncertain with SD=1 K, then the net warming PDFs for the central point are shown in Figure 2. The differences are surprisingly small. The Uniform and Narrow cases give a slightly narrower net warming.

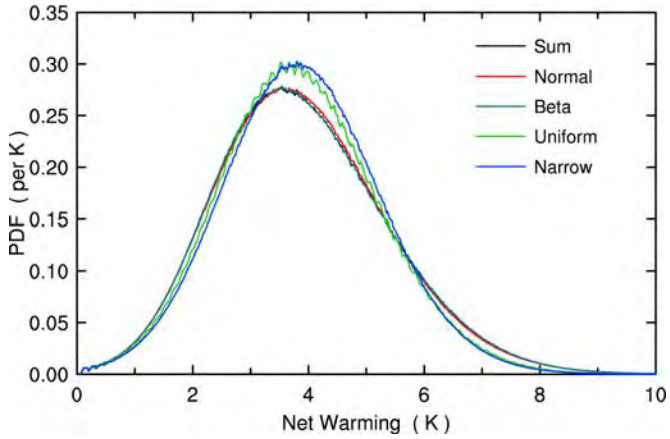

Figure 2. Probability distribution function for net warming at the point calculated from the five warming ratio PDFs and assuming the SD for global warming is 1K.

An intermediate case (SD=0.2 K) produces the net warming curves for the central point shown in Fig. 3. The PDFs more closely reflect the differences in Fig. 1.

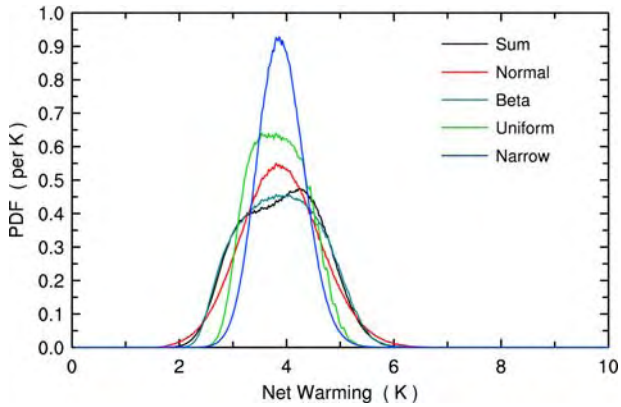

Figure 3. Probability distribution function for net warming at the point calculated from the five warming ratio PDFs and assuming the SD for global warming is 0.2 K.

3. Selecting climate change results based on model performance

Here we describe an assessment of models rainfall results for the Murray Darling Basin (MDB) region. This technique can be used to restrict the number of models contributing to the calculated PDFs described above.

23 AR4 model results (based on the A1B emissions scenario) were assessed. Several approaches were taken to determine the best models performing models with regard to Australia wide annual and seasonal rainfall. A set of best model results were selected as those with above median spatial correlation coefficients and those with below median root mean square errors. In addition to assessing the seasonal mean values, the models were also assessed in terms of their ability to reproduce the seasonal cycle of rainfall at several key locations, including the MDB. Finally, the results from the coarse resolution models were excluded since previous studies have highlighted the importance of horizontal resolution and the representation of topography as crucial to model rainfall.

The details of the full assessment are not shown here but, it is apparent that some simulations are clearly inferior, failing to adequately reproduce either the broad spatial patterns or the quantitative amounts. Of the 22 models, 7 were assessed to provide the best simulations of present day rainfall:
(GFDL-Cm2.0, ECHAM5, GISS-AOM, UKMO-HADcm3, MIROC3.2 (hires), GFDL-CM2.1 and UKMO-HADgem1).

Annual and seasonal percentage changes in rainfall for the period 2071-2100 relative to 1971-2000 based on the results using the A1B emissions scenarios (a mid-range scenario) were calculated for each model. These values are shown in Table 1.

Table 1. List of 22 model results for the projected percentage change in rainfall (2071 to 2100) vs (1971-2000). The top 7 selected models are highlighted.

		Percentage change in rainfall			
Model	Annual	Seasonal			
		DJF	MAM	JJA	SON
CSIRO-Mk3	-11.322	4.466	-15.344	-21.270	-30.431
GFDL-CM2.0	-12.410	28.991	3.562	-24.669	-34.333
MRI-CGCM2.3.2	-10.466	-23.397	-21.245	-23.397	-5.572
ECHAM5/MPI	-13.484	-5.725	15.261	-31.692	-32.450
GISS-ER	5.210	20.388	1.922	-17.495	-1.846
FGOALS-G1.0	-4.575	-3.917	-10.238	-5.016	-1.659
MIROC3.2(medres)	20.688	48.390	41.733	-11.238	-0.223
ECHO-G	22.783	59.088	22.942	-16.677	1.451
CCSM3	7.205	12.315	7.876	-10.856	15.790
GISS-AOM	-20.329	-28.843	19.923	-26.280	-29.721
UKMO-Hadcm3	-14.435	-7.082	6.650	-10.674	-40.274
GISS-EH	18.648	23.904	19.404	13.046	13.502
INM-cm3.0	-6.851	7.147	3.022	-19.065	-17.389
MIROC3.2(hires)	-6.016	5.458	6.496	-13.575	-25.254
CGCM3.1(t47)	11.343	6.238	14.308	15.988	8.202
GFDL2.1	-19.963	-1.245	-23.409	-46.104	-12.085
CGCM3.1(t63)	18.705	34.496	14.570	11.931	11.583
BCCR-BCM2	10.103	12.732	37.770	-12.632	5.467
CNRM-CM3	-7.372	7.360	18.003	-36.970	-35.549
IPSL-CM4	-33.637	-19.862	-31.908	-34.185	-52.639
UKMO-HADGEM1	-18.704	8.374	-28.881	-35.057	-30.272
PCM	-5.919	-7.968	-9.864	11.399	-16.497
22-model average	-3.2	8.2	4.2	-16	-14
22-model range	-33 to +23	-24 to +59	-31 to +42	-46 to +16	-53 to +16
Best 7 average	-15	-0.01	-0.06	-27	-29
Best 7 range	-20 to -6	-29 to +8	-29 to +20	-46 to -11	-40 to -12

The important result from this assessment is that the average changes from the best 7 models are more negative than the 22-model averages. Furthermore, this is not purely an artifact of the different sample sizes. T-statistics indicate that the best-7 sample results for rainfall and changes are significantly different to those of the remaining 15 models. For example, the chances that the 7-model average percentage change in annual rainfall (-15%) comes from the same population as the remaining 15 models is close to .001. In other words, the 7-best models form a distinctly different sub-set to

the other models. This is what we would expect if a poor simulation of present day climate is associated with an unreliable prediction of future climate.

These results need to be confirmed and recast into probabilities but it is apparent that the application of this new method paints a somewhat more pessimistic outlook for rainfall over the MDB into the future than previously indicated. We expect that it will be possible (Project 2.2.3b) to refine the projections for this region to better satisfy stakeholder expectations.

4. Summary

- Five different types of scaled warming PDF have been considered. Support for using each of these could be argued, although the uniform distribution, with no weighting of models is clearly outdated. The three other methods of fitting the spread of individual model results produce rather similar net warmings.

- A careful analysis of the performance of IPCC climate models at reproducing features of Australian rainfall has been undertaken. The results suggest that 7 (of the 23 assessed) should be accorded relatively high weightings when preparing PDFs.

The project objectives have been met and these findings will be used to generate the probabilistic information as described under Project 2.2.3b

Summary of methods and modifications (with reasons)
No modifications

Summary of links to other projects
The techniques that have been developed can now be applied to results for temperature and rainfall for the MDB and CMA regions as deliverables for Project 2.2.3b.

Recommendations for changes to work plan from your original table
Nil

Acknowledgements
This work was funded under the South East Australia Climate Initiative and the Australian Climate Change Science Program.

Publications arising from this project

Smith, I.N., Chandler, E., Suppiah, R and Watterson, I.G. (2007) Rainfall Projections: Are they really that uncertain? - results for the Murray Darling Basin. Abstract, Climate and Hydrology Symposium, Canberra, November 2007.

Watterson (2006) Some methods for specifying PDFs. CMAR Technical Note, 14 February, 2006.

Watterson, I.G. (2007) Calculation of probability functions for temperature and precipitation change under global warming. Abstract, Greenhouse2007.

Watterson, I.G. (2007) Calculation of probability density functions for temperature and precipitation change under global warming. Submitted to J.Geophys. Res.

References

Chandler, E. (2007) Reducing uncertainty in model results for Australian rainfall in the 21st century. *Abstract,* AMOS National Conference, Adelaide, February 2007.

CSIRO, 2001. Climate projections for Australia. CSIRO Atmospheric Research, Melbourne, 8 pp. http://www.dar.csiro.au/publications/projections2001.pdf

Suppiah, R., K. J. Hennessy, P. H. Whetton, K. McInnes, I Macadam, J. Bathols and J. Ricketts (2007) Australian climate change projections derived from simulations performed for the IPCC 4th Assessment Report. *Aus. Met Mag*. (in press).

Watterson, I. G. (2005) Climate change for the IPCC scenarios simulated by the IPCC multi-model ensemble: results scaled by global mean warming. *Internal report,* 24 May 2005.

Watterson (2006) Some methods for specifying PDFs. *CMAR note,* 14 February, 2006.

Watterson, I.G. (2007a) Simulation of climate and climate change by global models. *SEACI Project 2.1.5a report,* 23 November, 2006.

Watterson (2007b) Calculation of probability functions for temperature and precipitation change under global warming. *Journal of Geophysical Research* (submitted).

Whetton, P.H., McInnes, K.L., Jones, R.N., Hennessy, K.J., Suppiah, R., Page, C.M., Bathols, J., and Durack P. (2005) Climate change projections for Australia for impact assessment and policy application: A review. *CSIRO Technical Paper*. 001, Aspendale, Vic., CSIRO Marine and Atmospheric Research, 34p. http://www.cmar.csiro.au/e-print/open/whettonph_2005a.pdf

Whetton, P. H., Macadam, I., Bathols, J. M., and O'Grady, J. (2007). Assessment of the use of current climate patterns to evaluate regional enhanced greenhouse response patterns of climate models. Geophysical Research Letters, 34 (14): L14701, doi:10.1029/2007GL030025

Project Milestone Reporting Table

Develop improved regional projection techniques	Report produced.	30/6/07	70	Techniques for deriving probability functions at grid points over the regions of interest have been developed. The effect of model weighting on the mean response has been demonstrated to be significant and an important component in deriving the probability functions.	None

Appendix 1
Probabilistic Climate Change Projections for South East Australia: Surface Warming Examples

Ian G. Watterson

1. Introduction

We wish to provide improved methods of projecting climate change for Australia, building on the previous Climate Impact Group (CIG) approach described by Whetton et al. (2005). The main aim is to provide a confidence weighting throughout the range of change considered plausible, basing this on the data from simulations by a number of current climate models. For most quantities this means, in effect, a 'probability density function' (PDF) for the change variable. Several recent studies have provided such results based on various approaches and assumptions, often of considerable complexity. A new, relatively simple method, extending that of the CIG, was outlined in my previous note (Watterson, 2006). This is applied to a more realistic case here, to produce surface warming projections over south east Australia (specifically, the domain depicted in Figure 1). The models used and a simple estimation of weighting of them is presented in section 2. (I am able to make use of results prepared for both the SEACI and ACCSP modelling projects here.) Patterns of change (scaled by global mean warming) are considered in Section 3, and probabilistic scaled warming is presented, determined using five approaches. The distributions for net warming under three idealised global mean warming distributions are calculated and presented in Section 4.

2. GCM simulations of climate and climate change for South East Australia

In support of the 2007 Fourth Assessment Report on climate change by the IPCC, a major climate simulation project has been organised by the World Climate Research Program. Some 17 modelling centres from 9 countries have performed simulations of the period 1870-2100 and beyond, using their current climate models. The experiments include prescribed greenhouse gas (GHG) and aerosol changes based on observations to 2000, then following one of three SRES scenarios to 2100, with constant forcing thereafter. Data from some 22 models are currently being considered for the new CSIRO projections. This report considers only four individual models, but briefly compares these to the 'multi-model mean' (courtesy Julie Arblaster). The models are listed in Table 1. Preliminary data from the new version of CSIRO's current model 'Mk3.5' are included here. Results from HadGem and GFDL are courtesy of Janice Bathols and Ian Macadam.

Averages for both the full year and the four seasons over the period 1961-1990 have been formed for a number of quantities, including surface air temperature, precipitation and sea-level pressure. These are presented in my upcoming report for SEACI. A simple skill assessment of these quantities is shown in Fig. 2. All four models simulate both the area mean and local values quite well, in comparison to the 0.25° gridded observational data for temperature and precipitation from the Bureau of Meteorology. Data from ERA reanalyses are used as the observational fields for SLP.

Interestingly, the multi-model mean compares slightly better than the individual models, except that HadGem just beats it in two quantities. The ERA rainfall field suffers from well-known problems and scores no better than the models. Some bias may exist from using the averages of daily max and min temperatures as the observational field.

Consideration of an appropriate weighting of models is not the topic of this note. Ideally, this could be based on the (hypothetical) ability of models to simulate the local climate change in a particular field, scaled (or normalised) by the global mean warming. For illustration, we consider here the mean of the seasonal averages in Fig. 2, averaged over the three quantities, as a weight. Dividing by the sum of the four results gives the numbers in Table 1. This rather uniform set of weights will be used for all grid points in the example presented shortly.

Table 1. Models considered in the study, the weight assigned to them and the global mean warming to 2100 under A1B.

Model Name	**Origin**	**Weight**	**Warming (K)**
Mark 3.0	CSIRO Atmospheric Research	0.234	2.21
Mark 3.5	CSIRO Atmospheric Research	0.239	3.43
HadGem	UK Meteorological Office	0.273	3.53
GFDL 2.1	Geophys. Fluid. Dyn. Lab., USA	0.254	2.76
MMM	Multi-Model Mean		2.89

In the multi-model means, the ‘Murray Darling Basin’ regional annual mean change in temperature divided by the global mean is between 1.105 and 1.158 for all SRES scenarios and time periods. Thus, there appears to be little systematic bias in using scaled patterns over the region (see also Watterson, 2005).

Changes from 1976 to 2100 have been determined by linear interpolation between the 1961-90 and 2071-2100 averages. Global mean warmings for this span under the A1B scenario from the models are given in Table 1. (Note that there is no account of control model drift in these values, which would boost the Mk3.0 result to one close to the MMM result.) Maps of the scaled change of temperature for summer (DJF), interpolated to a common 1° grid, are shown in Fig. 1.

The individual model results are determined from land points only (1a to 1d). As described by Watterson et al. (2006) simulations at 0.5° by CCAM show that a sharp drop in warming occurs at coasts, on going from land to ocean. It would seem wise to avoid linear interpolation between land and ocean points as a means of producing values near the real coastline. To assist in producing interpolated values nearer the coast, the model fields are first interpolated to a double grid, using extrapolation to the edges of coastal land squares. The final 1° grid fields are plotted using cell colouring. In fact, the HadGem and (apparently) GFDL models allow squares with fractional surface types. The relatively low values on points that extend beyond the true coast are a result of this. Averaging over the four models (with weights) avoids these values if points with less than four model results are omitted (compare the 1e and 1f maps). A weighted average of results simply interpolated from the full grid is in 1g. The difference over land is rather small in this case, due to the relatively high resolution of the models (2° or better). The simple average over all 22 models, 1h, produces less

abrupt land-sea contrast, partly due to differing and often coarser model grids and coastlines.

3. Distributions for scaled change

In the previous note, a number of methods for generating a PDF for scaled change of a certain quantity at a single point were described. These are illustrated in Fig. 3, using data for warming at the central point of the map, 142°E and 31°S. Allowing for statistical uncertainty, the true value for each model (from multiple runs) is assumed to be from a simple normal PDF centred on the sample value. The uncertainty is determined from that appropriate to differences of two 30-y means, assuming these follow from the interannual standard deviation field, then scaled. The available SD field from Mk3.0 is used for all models here, with the result scaled by 3K. The four sample change ratios here are 1.23, 1.42, 1.02 and 1.55. The common uncertainty SD is 0.11. The weighted sum of the four individual distributions is the 'Sum' PDF in Fig 1. The normal distribution fitted to this Sum curve is also shown (as Normal). The range of ratio values allowed here extends from the point where the corresponding cumulative distribution (CDF) is 0.001 to the point where it is 0.999. 1000 values are used to provide close representation of all the curves. These will differ for each grid point –there being no need for them to be common here.

The beta distribution fit to the Sum curve is also shown. Here the end points (two of the four parameters) give the 0.01 and 0.99 values of the CDF of Sum. The steep sides of Sum here lead to sharply dropping sides of Beta. The Uniform distribution is between the smallest and largest of the four change ratios. The choice of second smallest and largest (which would be unwise for four values) would match the original CIG approach.

The final curve 'Narrow' is a normal fit to Sum, but with the SD reduced by the square root of the 'effective N'. This is the number of models, with allowance for uneven weighting, being the inverse of the sum of the squared weights. This distribution would be appropriate if one considered the various model results to be a sample from a normal distribution centred on the 'true' change. It would represent a plausible distribution for the 'true' value, whose uncertainty will be smaller the more models are used, as in standard statistical theory.

A range of statistics from each of these distributions can be determined. The means match that from the original model results -except in the Uniform case. The SDs vary somewhat, being smallest for Narrow, of course. Percentiles can be readily determined from the CDFs.

Applying the methods to every grid point with four model (land) values produces a map of means that matches 1f (even Uniform is very close). Plotted in Fig. 4 are the 10, 50 and 90 percentiles from all five cases. As anticipated from Fig. 3 the 10 to 90 range is usually smaller for Uniform and Narrow than for the other three.

4. Net warming for 2100

As in the CIG method, the patterns of scaled warming need to be combined with a global mean warming distribution to produce a net change. As described in the

previous note, the assumption is made that the scaled local change ‘x’ and the global warming ‘T’ are considered two independent variables. The joint distribution function is simply the product of the two PDFs. Statistics of the net local change can be determined numerically from this joint function.

Consider first the trivial case, where one proposes that the global warming has reached a single specific amount. For the A1B scenario in 2100, a value around 3 K is suggested by the models (Table 1). Suppose for simplicity it is exactly 3K. Then the joint PDF for the local warming is only trivially different from the scaled warming PDF, and all the statistics correspond to those from section 3, with a factor of 3 K. For instance, the maps in Fig. 4 apply to the net case, but with the scale amplified to range from 1.2 K to 6 K.

An idealised PDF that better reflects the uncertainty in global warming in this case, which I used previously, is illustrated in Fig. 5 –the SD=1K case. It is necessary to discretise this normal distribution, and 100 T points seem adequate. Now if the local warming ratio is a single value, say 1, the joint distribution is again simple. The net warming distribution is the same of the global result in Fig. 5.

For the more general case additional calculations are needed. Two methods were used previously. One is a straight forward evaluation of the joint function at each x and T step. This gives 100000 values of probability, each corresponding to a net warming P simply given by xT. Ordering these by P allows a simple conversion to a CDF as a function of P. The second method makes use of the simple form for P, and the separate nature of the joint function. This appears to be computationally more efficient by a factor of about 10.

The net warming PDFs for the central point, determined for the SD=1 global warming case and each scaled case, are shown in Fig. 6. The differences are surprisingly small. The Uniform and Narrow cases give a slightly narrower net warming. Performing the calculation at every grid point leads to the maps shown in Fig. 7. Again, there is very little difference across the five for the 10, 50 and 90 percentiles shown.

The similarity across the five cases is due to the scaled warming PDFs being all relatively narrow, in comparison with the global warming one. A case intermediate between the SD=1 case and the single T case above is for the SD = 0.2 curve shown in Fig. 5. This produces the net warming curves for the central point shown in Fig. 8. The PDFs more closely reflect the differences in Fig. 3.

5. Summary

This note applies the method previously described for generating PDFs for scaled warming and net warming to points over SE Australia. The range of possible results at each point is evident from the maps of 10 and 90 percentile statistics that are generated. The choice of the four models and their weighting used here is only for example purposes.

As previously, five different types of scaled warming PDF are considered. Support for using each of these could be argued, although the uniform distribution, with no weighting of models is clearly outdated. The three other methods of fitting the spread

of individual model results produce rather similar net warmings, in practice. The Beta case has the advantage of allowing a non-zero skewness and a finite range using only four parameters. Given the popularity of Bayesian methods, which (as I understand it) lead to narrowing ranges as the number of models increases, the Narrow case should also be considered. Fortunately, evaluation of all five cases, even for multiple T scenarios, seems quite feasible. Application of the method to a larger set of models and other variables is recommended.

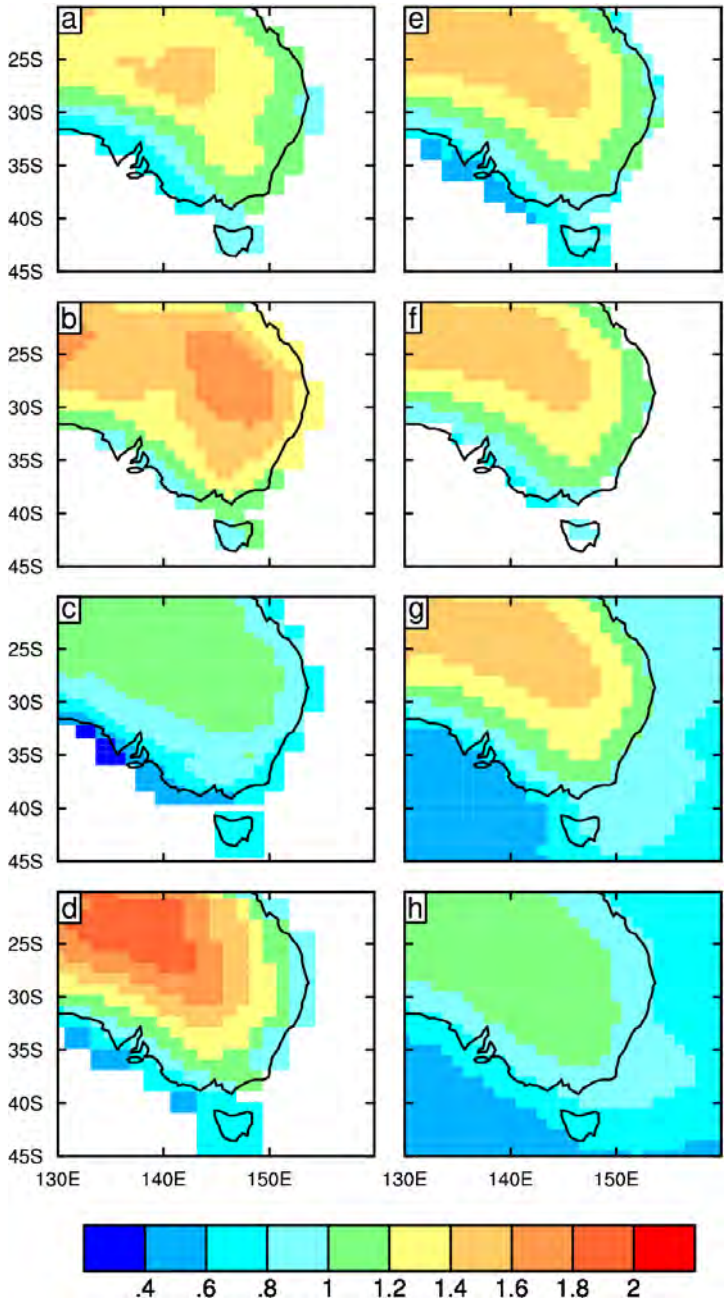

Fig. 1. Change in mean surface air temperature over SEA land divided by global annual mean change for DJF, between years 1976 and 2100, under the A1B scenario, from (a) Mk3.0, (b) Mk3.5, (c) HadGEM, (d) GFDL2.1, (e) weighted mean of one to four models, (f) weighted mean of all four models, (g) weighted mean of four models from land and sea values, and (h) AR4 multi-model mean.

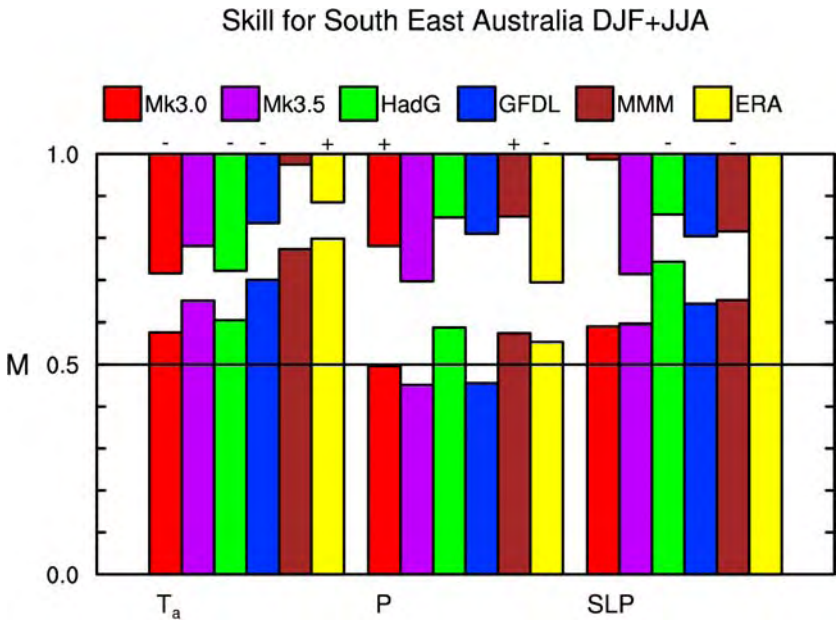

Fig. 2 Histogram representing skill of four models and the MMM in reproducing observational climatological means using data from SEA land for quantities surface air temperature (T_a), precipitation (P) and sea-level pressure (SLP). Bars up from 0 are the M score, bars down from 1 are the M score representing the mean bias over SEA. Both are averaged over the DJF and JJA results. A + or – symbol is shown when the mean bias is of the same sign in both seasons. An additional observational result from ERA40 (1958-2001) is also considered. For SLP, the M score for ERA is unity, as ERA is used as the observed. All data were interpolated to the common BOM grid, and land points in the plotted domain used.

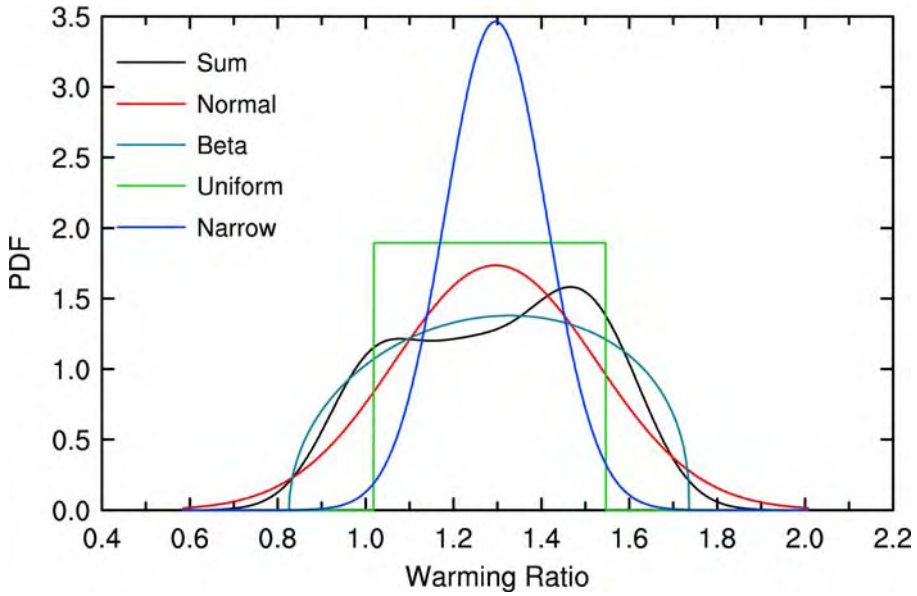

Fig. 3. Probability distribution function for the warming ratio at point 142°E, 31°S calculated from the four models, using five methods, as in key.

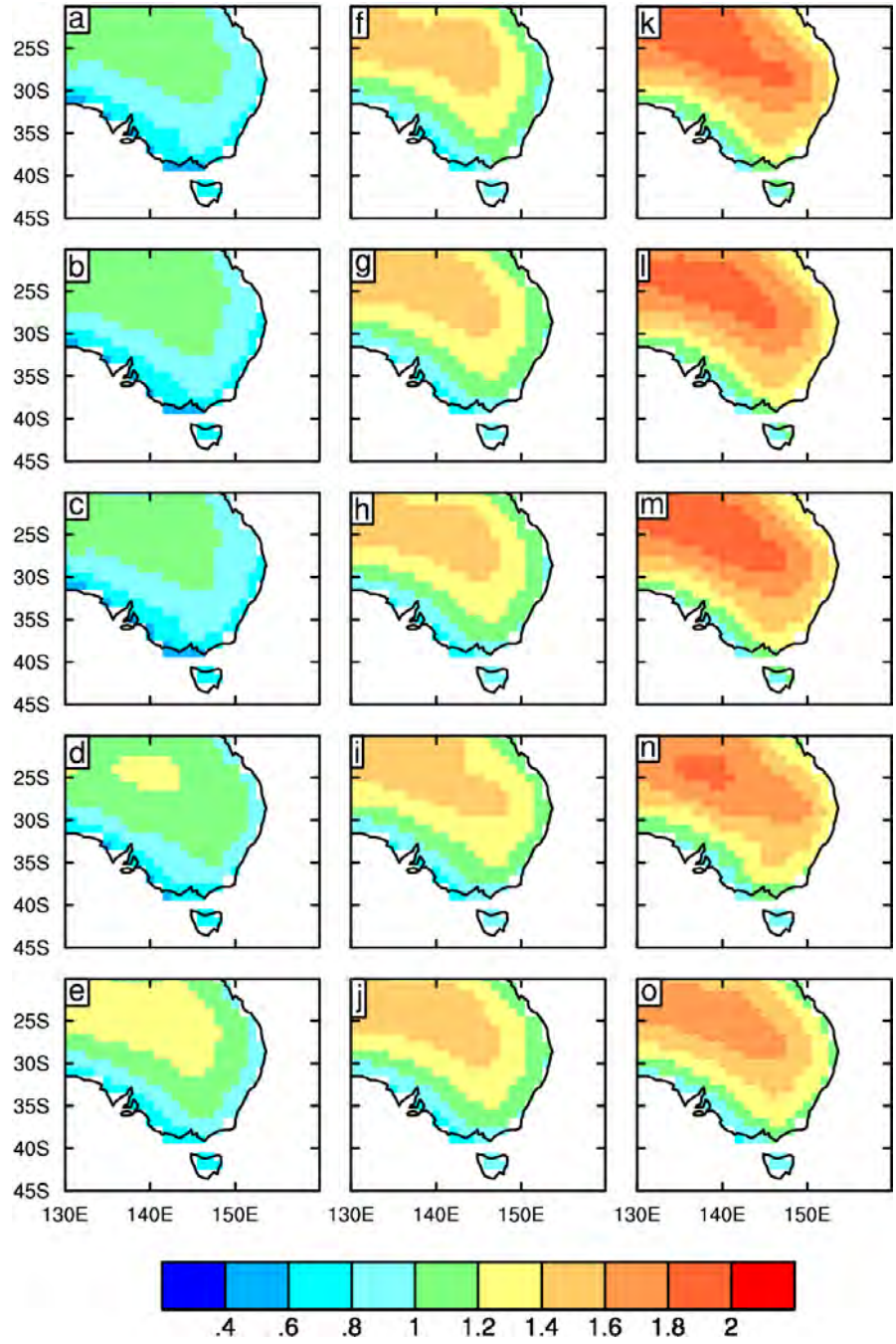

Fig. 4. Maps of percentiles of the warming ratio from all distributions (top to bottom) Sum, Normal, Beta, Uniform, and Narrow: Left column 10%, Middle column 50% and right column 90%.

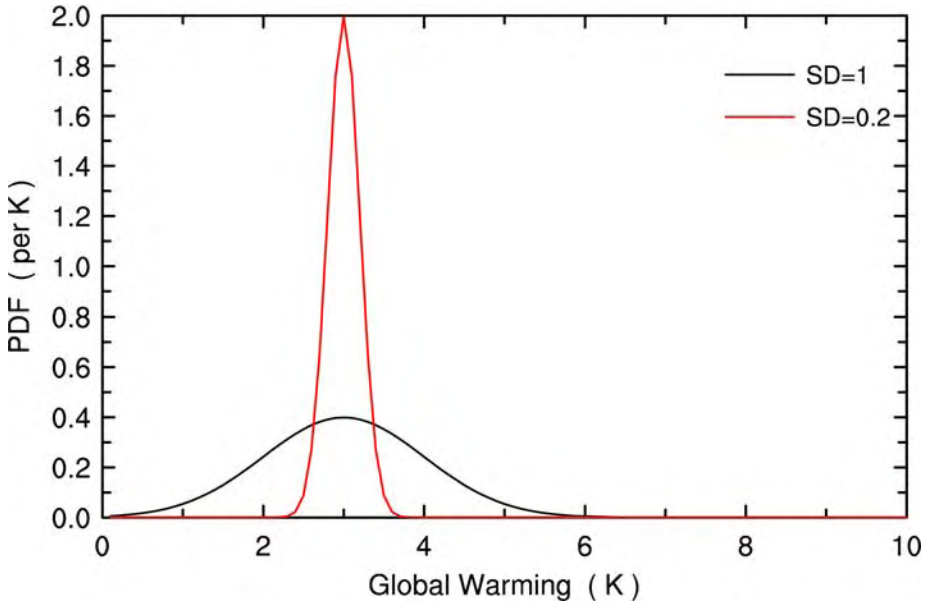

Fig. 5. Idealised distribution of global mean warming, based on the normal distribution with 3 K and SD 1 K or 0.2 K.

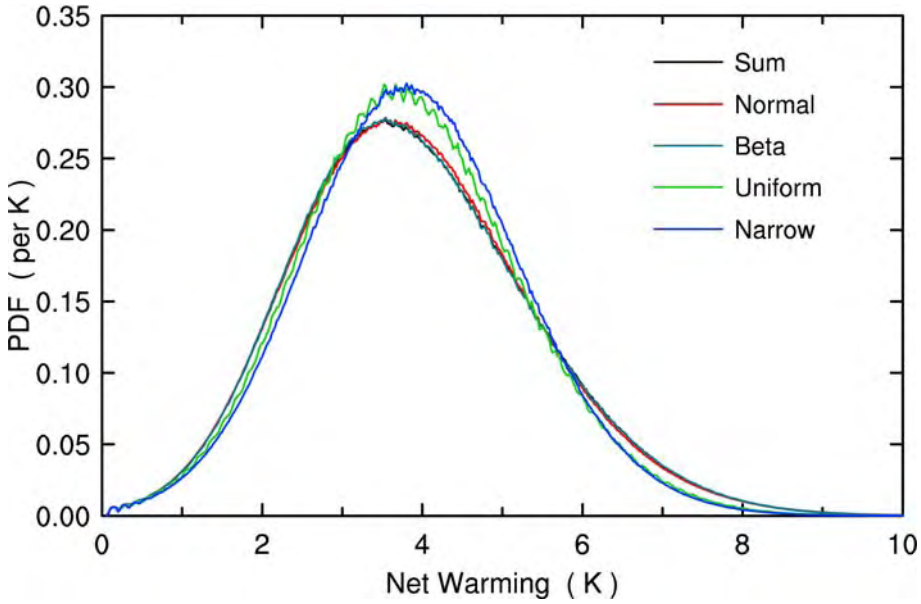

Fig. 6. Probability distribution function for net warming at point 142°E, 31°S calculated from the five ratio PDFs (as in the key) and the SD 1K global warming PDF.

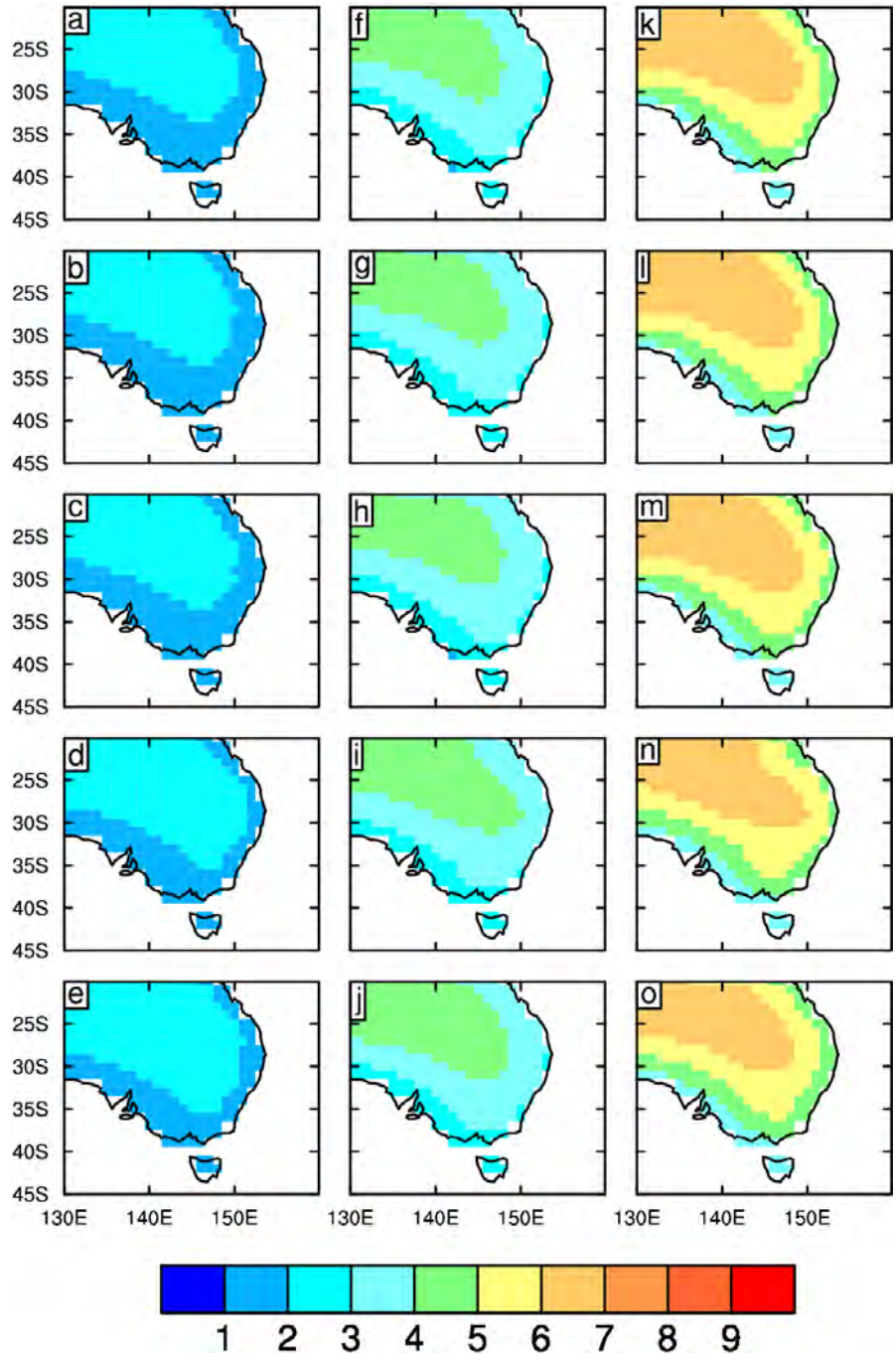

Fig. 7. Maps of percentiles of net warming from all distributions (top to bottom) Sum, Normal, Beta, Uniform, and Narrow: Left column 10%, Middle column 50% and right column 90%.

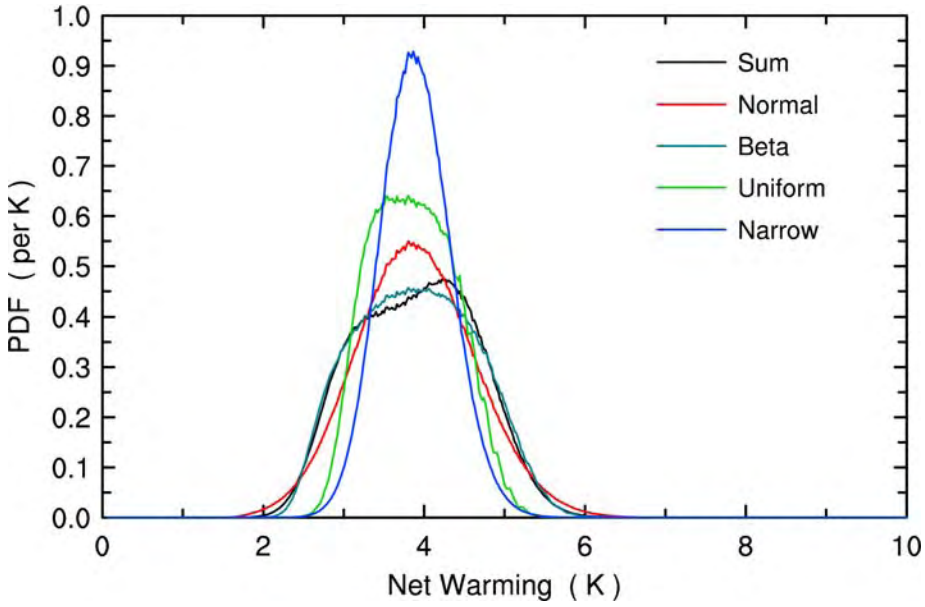

Fig. 8. Probability distribution function for the net warming at point 142°E, 31°S calculated from the five ratio PDFs (as in the key) and the SD 0.2 K global warming PDF.

References

Watterson, I. G. (2006) Some methods for specifying PDFs. *Internal report, dated 14-02-06.*

Watterson, I. G. (2005) Climate change for the IPCC scenarios simulated by the IPCC multi-model ensemble: results scaled by global mean warming. *Internal report, dated 24 May 2005.*

Watterson, I. G., J. McGregor, and K. Nguyen (2006) Influence of winds on changes in extreme temperatures near Australian coasts, as simulated by CCAM. *Abstract for the AMOS National Conference, Adelaide, February 2007*

Whetton et al. (2005) Australian climate change projections for impact assessment and policy application: A review. *CMAR Res. Papr. 1*.

For details on the CSIRO Mk3 and Mk3.5 simulations, see cherax.hpsc.csiro.au/users/dix043/mk3runs/

For the full IPCC dataset, see http://www-pcmdi.llnl.gov/ipcc/about_ipcc.php

Appendix 2
Selecting climate change results based on model performance
Ian Smith and Elise Chandler

It can be argued that weighting models is not ideal since it implies that the results from better performing models can be diluted when combined with the results of poorer performing models. Chandler (2007) provides a preliminary analysis of projections by deliberately ignoring all but the best performing models over the Australian region. Here we describe some further results based on this technique as applied to the MDB region.

Since rainfall is one of the most difficult variables to simulate accurately, we argue that a reliable projection of rainfall must be accompanied by a reasonable simulation of present day rainfall. An assumption here is that a model must, by definition, accurately simulate a number of variables (moisture content, temperatures, winds, pressure etc.) correctly if it is to simulate rainfall correctly. Secondly, we also argue that , because Australia is a continent encompassing a wide range of climate regimes, that a regional projection is more likely to be reliable if the model can capture the variability in space over the wider Australian region. Thirdly, we also argue that, in addition to accurately simulating the means and spatial variability, the ability to simulate the seasonal cycle also provides an important performance measure.

23 AR4 model results (based on the A1B emissions scenario) were assessed. Several approaches were taken to determine the best models performing models. The first of these involved using threshold values for the correlation coefficient and RMSE. Following Suppiah *et al*. (2004), a threshold value of 0.7 chosen as the minimum value for the spatial correlation coefficient. A set of best model results were then selected as those with above median correlation coefficients and those with below median RMS errors. In addition to assessing the seasonal mean values, the models were also assessed in terms of their ability to reproduce the seasonal cycle of rainfall at several key locations, including the MDB. Finally, the results from the coarse resolution models were excluded since previous studies have highlighted the importance of horizontal resolution and the representation of topography as crucial to model rainfall.

The details of the full assessment are not shown here but, it is apparent that some simulations are clearly inferior, failing to adequately reproduce either the broad spatial patterns or the quantitative amounts. In particular, the models IPSL-cm4, BCCR-BCM2, GISS-EH, GISS-AOM, and FGOALS-G1.0 performed poorly in regions of high rainfall (not shown). At the shorter seasonal timescale, spring and autumn were the seasons most difficult to simulate and this proved to highlight the better performing models.

Of the 23 models, 7 were assessed to provide the best simulations of present day rainfall:
GFDL-Cm2.0
ECHAM5
GISS-AOM
UKMO-HADcm3

MIROC3.2 (hires)
GFDL-CM2.1 and
UKMO-HADgem1.

Annual and seasonal percentage changes in rainfall for the region shown in Figure 1 for the period 2071-2100 relative to 1971-2000 based on the results using the A1B emissions scenarios (a mid-range scenario) were calculated for each model. These were then divided by the same model's estimate of global temperature increase over this period to arrive at a percentage change per degree of global warming. These values are shown in Table 1.

.

Figure 1. Map showing grid points used to define the Murray-Darling river basin.

Table 1. List of 23 model results for the projected percentage change in rainfall (per degree of global warming) over the MDB region. The top 7 selected models are highlighted. The 22-model average shown excludes the results for BCCR-BCM2.

		Percentage change in rainfall				
	Model	Annual	Seasonal			
			DJF	MAM	JJA	SON
1	CSIRO-Mk3	-11.322	4.466	-15.344	-21.270	-30.431
2	GFDL-CM2.0	-12.410	28.991	3.562	-24.669	-34.333
3	MRI-CGCM2.3.2	-10.466	-23.397	-21.245	-23.397	-5.572
4	ECHAM5/MPI	-13.484	-5.725	15.261	-31.692	-32.450
5	GISS-ER	5.210	20.388	1.922	-17.495	-1.846
7	FGOALS-G1.0	-4.575	-3.917	-10.238	-5.016	-1.659
8	MIROC3.2(medres)	20.688	48.390	41.733	-11.238	-0.223
9	ECHO-G	22.783	59.088	22.942	-16.677	1.451
10	CCSM3	7.205	12.315	7.876	-10.856	15.790
11	GISS-AOM	-20.329	-28.843	19.923	-26.280	-29.721
12	UKMO-Hadcm3	-14.435	-7.082	6.650	-10.674	-40.274
13	GISS-EH	18.648	23.904	19.404	13.046	13.502
14	INM-cm3.0	-6.851	7.147	3.022	-19.065	-17.389
15	MIROC3.2(hires)	-6.016	5.458	6.496	-13.575	-25.254
16	CGCM3.1(t47)	11.343	6.238	14.308	15.988	8.202
17	GFDL2.1	-19.963	-1.245	-23.409	-46.104	-12.085
18	CGCM3.1(t63)	18.705	34.496	14.570	11.931	11.583
~~19~~	~~BCCR-BCM2~~	~~10.103~~	~~12.732~~	~~37.770~~	~~-12.632~~	~~5.467~~
20	CNRM-CM3	-7.372	7.360	18.003	-36.970	-35.549
21	IPSL-CM4	-33.637	-19.862	-31.908	-34.185	-52.639
22	UKMO-HADGEM1	-18.704	8.374	-28.881	-35.057	-30.272
23	PCM	-5.919	-7.968	-9.864	11.399	-16.497
	22-model average	-3.2	8.2	4.2	-16	-14
	22-model range	-33 to +23	-24 to +59	-31 to +42	-46 to +16	-53 to +16
	Best 7 average	-15	-0.01	-0.06	-27	-29
	Best 7 range	-20 to -6	-29 to +8	-29 to +20	-46 to -11	-40 to -12

The important result from this assessment is that the average changes from the best 7 models are more negative than the 22-model averages. Furthermore, this is not purely an artefact of the different sample sizes. T-statistics indicate that the best-7 sample results for rainfall and changes are significantly different to those of the remaining 15 models. For example, the chances that the 7-model average percentage change in annual rainfall (-15%) comes from the same population as the remaining 15 models is close to .001. In other words, the 7-best models form a distinctly different sub-set to the other models. This is what we would expect if a poor simulation of present day climate is associated with an unreliable prediction of future climate.

These results need to be confirmed and recast into probabilities but it is apparent that the application of this new method paints a somewhat more pessimistic outlook for rainfall over the MDB into the future than previously indicated. We expect that it will be possible (Project 2.2.3b) to refine the projections for this region to better satisfy stakeholder expectations.

References

Chandler, E. (2007) Reducing uncertainty in model results for Australian rainfall in the 21st century. Abstract, AMOS National Conference, Adelaide, February 2007.

CSIRO, 2001. Climate projections for Australia. CSIRO Atmospheric Research, Melbourne, 8 pp. http://www.dar.csiro.au/publications/projections2001.pdf

Smith (2007) Regional rainfall projections refining model-based estimates using observed trends. Abstract, IUGG, Perugia, Italy, July 2007.

Suppiah, R., K. J. Hennessy, P. H. Whetton, K. McInnes, I Macadam, J. Bathols and J. Ricketts (2007) Australian climate change projections derived from simulations performed for the IPCC 4th Assessment Report. *Aus. Met Mag. (accepted).*

Watterson (2005) CMAR Research Paper 1.

Watterson, I.G. (2006) Simulation of climate and climate change by global models. SEACI Project 2.1.5a report (23 November, 2006).

Watterson (2007) Calculation of probability functions for temperature and precipitation change under global warming. (submitted to Journal of Geophysical Research).

Whetton, P.H., McInnes, K.L., Jones, R.N., Hennessy, K.J., Suppiah, R., Page, C.M., Bathols, J., Durack P. (2005) Climate change projections for Australia for impact assessment and policy application: A review. CSIRO Technical Paper. 001, Aspendale, Vic., CSIRO Marine and Atmospheric Research, 34p. http://www.cmar.csiro.au/e-print/open/whettonph_2005a.pdf

Whetton, P. H., Macadam, I., Bathols, J. M., and O'Grady, J. (2007). Assessment of the use of current climate patterns to evaluate regional enhanced greenhouse response patterns of climate models. Geophysical Research Letters, 34 (14): L14701, doi:10.1029/2007GL030025.